

Analysis of Alzheimer's Disease Progression in Structural Magnetic Resonance Images

MAHANAND B.S., ASWATHA KUMAR M.*

Department of Information Science and Engineering

Sri Jayachamarajendra College of Engineering, Manasagangotri, Mysore 570 006

*Department of Information Science and Engineering

M S Ramaiah Institute of Technology, M S Ramaiah Nagar, Bangalore 560 054

INDIA

bsmahanand@sjce.ac.in maswatha@yahoo.com

Abstract: Structural magnetic resonance imaging (MRI) of the brain is an increasingly useful tool in the study of neurodegenerative diseases. MRI is currently the fastest developing medical imaging modality which is applied to an increasingly number of different medical diagnostic situations. Serial acquisition structural images of a subject's brain are acquired over time offers opportunities to monitor the progression of tissue volume changes in fine detail at all anatomical locations. As a result, the analysis of structural MRI data has been an active area of image analysis research for many years especially in early diagnosis, tracking of disease progression, which makes it possible to investigate how, for instance, a patient responds to treatment. The aim of the paper is to investigate and analyze brain tissue changes in Alzheimer's disease using non-rigid medical image registration and statistical analysis techniques. In our proposed approach, first the source and the target images are affinely registered to correct global differences between the images and then non-rigid registration based on free-form deformation using B-spline approximation is performed on the images. The resulting displacement values from the non-rigid registration are further investigated for deformation in the entire brain to detect typical deformation patterns. Finally, statistical method namely t-test is performed for analysis of the results. The initial results indicate that the tissue volume change in the brain occurs predominantly in the hippocampus of the brain.

Key-Words: Magnetic resonance imaging, Image registration, Free-form deformation, Alzheimer's disease, Statistical analysis, T-test.

1 Introduction

Medical imaging has gone through a revolution since the advent of X-ray computed tomography imaging in early seventies and the introduction of other imaging modalities such as magnetic resonance imaging, positron emission tomography, etc in the later years. Image Registration is a fundamental task in many modern Image Processing and Computer Vision tasks. Image registration plays a vital role in current clinical practice and biomedical research. Various image registration applications include multispectral classification, environmental monitoring, change detection, target

localization, tumor growth detection and lung cancer screening [1]. Because of its importance in various application areas and its complicated nature, image registration has been the topic of much recent research [2, 3, 4, 5, 6].

The application of automated volumetric non-rigid registration techniques to brain shape analysis is emerging as a powerful approach to automated computational neuroanatomy [7, 8, 9, 10, 11]. Non-rigid registration essentially aims to capture all geometric differences between scans in terms of a spatial transformation. By estimating the transformation to bring individual brain structures into

correspondence with a common anatomical space, it allows spatial mapping of local shape differences over the brain across a population.

Alzheimer's disease (AD) is arguably one of the greatest threat to public health in the 21st century. AD is a progressive disorder that leads to problems with memory, learning, judgement, communication, and the basic abilities needed for independent living. At present, researchers know of no single cause, nor of a cure. Imaging studies have become a priority in Alzheimer's disease research as they can be used to evaluate treatments that may slow or delay the disease process [12,13].

The proposed work investigates on the application of non-rigid medical image registration and statistical analysis techniques to serially acquired MRI scans, with the aims of identifying tissue volume changes in the brains of AD patients and to distinguish differences between patients and controls. Differences between groups of subjects may be relevant to diagnosis, tracking of disease progression, and monitoring of potential disease-modifying treatments.

2 Image Registration

Image registration is the process of overlaying images of the same scene taken at different times, from different viewpoints, and/or by different sensors. In other words it is a process of finding a transformation that aligns one image to another. Image registration is a fundamental task in image processing. Virtually all large image analysis systems which evaluate images uses image registration techniques as the intermediate step [14]. The first step is to find a correspondence between voxel in the source image with the pixels in the target image. More precisely the goal of image registration is to find a correspondence function or mapping F that takes each spatial coordinate \vec{x}_t and returns

a coordinate \vec{x}_s for source image. Now we have

$$\vec{x}_s = F(\vec{x}_t) \quad (1)$$

Once the transformation function is obtained, the source image may be brought in to registration with the target image by warping the source using interpolation. A typical categorization of registration techniques based on transformation types are classified into rigid, affine and non-rigid registrations. The rigid registration allows translation and rotation. The normalized shape attributes are altogether preserved and the process is usually concerned merely with some common alignment. The Affine registration allows the image to stretch and skew along at least one axis or dimension, but not necessarily all (so that homogeneous scaling can be broken). Despite the fact that previously essential constraints are broken, all lines that were parallel remain parallel after the transformation is applied. All other valid transformations fall into non-rigid registration category. In principle, no inviolable constraints are in place, but quite clearly a non-rigid transformation attempts to preserve some of the primary structure of the image while avoiding tearing and folding. This means that each voxel in the range must map to another and no voxel is left undefined.

The main difference between rigid and non-rigid registration techniques is the nature of the transformation. The goal of rigid registration is to find the six degrees of freedom (3 rotations and 3 translations) of a transformation which maps any point in the source image into the corresponding point in the target image. An extension of this model is the affine transformation model which has up to twelve degrees of freedom and allows for scaling and shearing. By adding additional degrees of freedom, such a linear transformation model can be extended to non-linear transformation models.

Free-form deformations (FFD) based on locally controlled functions such as B-splines are a powerful tool for modeling 3D

deformable objects [15] and have been used successfully for image registration [16, 17, 18]. The basic idea of FFDs is to deform an object by manipulating an underlying mesh of control points. The resulting deformation controls the shape of the 3D object and produces a smooth and continuous transformation.

In our proposed approach, non-rigid registration based on FFD using B-spline approximation has been performed on the 3D brain MR images. The non-rigid registration algorithm moves the control points, tissue motion is described by FFD using B-spline approximation between the control points. In contrast to other methods, spline-based FFDs require a regular mesh of control points with uniform spacing. The control point spacing determines the flexibility of the grid. FFD using B-spline approximation was previously evaluated for the registration of 3D breast MR images [16] and of 3D brain MR images [19].

A spline-based FFD is defined on the image domain

$$\Omega = \{(x, y, z) | 0 \leq x < X, 0 \leq y < Y, 0 \leq z < Z\} \quad (2)$$

Let Φ denotes an $n_x \times n_y \times n_z$ mesh of control points $\phi_{i, j, k}$ with uniform spacing δ . In this case the displacement field u defined by the FFD can be expressed as the 3D tensor product of the familiar 1D cubic B-splines [20]

$$u(x, y, z) = \sum_{l=0}^3 \sum_{m=0}^3 \sum_{n=0}^3 \theta_l(u) \theta_m(v) \theta_n(w) \phi_{i+l, j+m, k+n} \quad (3)$$

Where

$$i = \left\lfloor \frac{x}{\delta} \right\rfloor - 1, j = \left\lfloor \frac{y}{\delta} \right\rfloor - 1, k = \left\lfloor \frac{z}{\delta} \right\rfloor - 1 \quad (4)$$

$$u = \frac{x}{\delta} - \left\lfloor \frac{x}{\delta} \right\rfloor, v = \frac{y}{\delta} - \left\lfloor \frac{y}{\delta} \right\rfloor, w = \frac{z}{\delta} - \left\lfloor \frac{z}{\delta} \right\rfloor \quad (5)$$

and θ_l represents the l th basis function of the B-spline

$$\begin{aligned} \theta_0(s) &= (1-s)^3 / 6 \\ \theta_1(s) &= (3s^3 - 6s^2 + 4) / 6 \\ \theta_2(s) &= (-3s^3 + 3s^2 + 3s + 1) / 6 \\ \theta_3(s) &= s^3 / 6 \end{aligned} \quad (6)$$

In contrast to thin-plate splines [21], B-splines are locally controlled, which makes them computationally efficient even for a large number of control points. In particular, the basis functions of cubic B-splines have a limited support, i.e., changing control point affects the transformation only in the local neighborhood of that control point.

3 Deformation Field Analysis

First, source and target images are affinely registered with 12 degrees of freedom. The purpose of doing affine registration is to correct for global differences between the images. Then the non-rigid registration of the images is performed to produce the displacement values throughout the brain for each voxel in the image. The resulting displacement map can be used to investigate deformation in the entire brain and to detect typical deformation patterns.

The non-rigid registration algorithm results in a 3D deformation field D which is mathematically defined as a vector field $D: R^3 \rightarrow R^3$ and maps a point $p_{source}(x, y, z)$ from the source image to the target image $p_{target} = D(p_{source})$. Usually the deformation field is visualized as a displacement field. This field represents the displacement of each point p and is defined on the basis of the deformation field:

$$D(p) = p + d(p) \quad (7)$$

The Jacobian operator can be used to measure local relative tissue volume change throughout the brain. It is defined at the point p as the determinant of the Jacobian matrix of the deformation field.

$$Jac_p(D) = \begin{pmatrix} \frac{\partial D_x}{\partial x} & \frac{\partial D_x}{\partial y} & \frac{\partial D_x}{\partial z} \\ \frac{\partial D_y}{\partial x} & \frac{\partial D_y}{\partial y} & \frac{\partial D_y}{\partial z} \\ \frac{\partial D_z}{\partial x} & \frac{\partial D_z}{\partial y} & \frac{\partial D_z}{\partial z} \end{pmatrix} \quad (8)$$

The Jacobian operator relates an elementary volume δV_{source} in the source image to the corresponding deformed volume δV_{target} in the target image

$$\delta V_{target} = Jac_p(D) \cdot \delta V_{source} \quad (9)$$

An intuitive way of representing shape information is to consider only relative volumes [22, 23]. Relative volumes can be represented by

$$V_{relative} = \det(J + I) \quad (10)$$

where I is a 3×3 identity matrix. Adding the identity matrix is done to ensure that an identity deformation has $V_{relative} = 1$. If $V_{relative} > 1$, the volume of the source is larger than the target and vice versa for $V_{relative} < 1$. We apply the Jacobian operator to the deformation field determined by the non-rigid algorithm to analyze the local volume change for each point in the image.

4 Statistical Analysis

The t-test is one of the simplest and most commonly used statistical methods [24]. The single-sample t-test concerns a hypothesis on the mean of a sample; the two-sample t-test considers the difference in means between two groups. The paired t-test is appropriate when the observations in two samples are in correlated pairs, as for example when a single quantity is measured on two occasions, and hence is important in cross-sectional and longitudinal studies. In our proposed approach, student's t-test is used to analyze the statistically significant localized differences between patient and control groups. T-test is applied on the each of the relative volume voxel and tested cross-sectionally across the subjects for significance.

5 Results

The Alzheimer's disease Neuroimaging Initiative(ADNI) data set from Laboratory of Neuro Imaging, University of California Los Angeles is used in our study [25]. The two time-point (screening and 6 months) data-set of T1-weighted MR volumes of 41 AD patients and 51 healthy controls is used in our study. Whole brain T1-weighted 3D MPRAGE (magnetization-prepared rapid-acquisition gradient echo) data sets were acquired in the sagittal plane using both GE Signma T 1.5 and Siemens T 1.5 Symphony MRI systems. The acquired volumes had dimensions of 256 x 256 x 166, with slice thickness of 1.2 mm.

Each image in the ADNI dataset has undergone specific image preprocessing correction steps. These corrections include gradwarp, B1 non-uniformity and N3. Gradwarp is a system specific correction of image geometry distortion due to gradient non-linearity. The degree to which images are distorted due to gradient non-linearity varies with each specific gradient model. It is anticipated that most users would want to use images which have been corrected for gradient non-linearity distortion in analyses. B1 non-uniformity correction procedure employs the B1 calibration scans noted in the protocol above to correct the image intensity non-uniformity that results when RF transmission is performed with a more uniform body coil while reception is performed with a less uniform head coil. N3 is a histogram peak sharpening algorithm which is applied to all images. It is applied after grad warp and after B1 correction for systems on which these two correction steps are performed. N3 will reduce intensity non-uniformity due to the wave or the dielectric effect at 3T. 1.5T scans also undergo N3 processing to reduce residual intensity non-uniformity.

To avoid influence from both the highly deformable soft tissue areas around the brain and the skull, the part of the image that contains the brain needs to be extracted from the rest of the image. For this purpose, a simple and most widely used

segmentation method namely brain extraction tool (BET) [26] is used on the dataset. BET takes an image of a head and removes all the non brain parts of the image. It uses surface model approach, to robustly and accurately carry out the segmentation without user intervention in short duration of time. BET results in image volumes containing only gray matter, white matter and internal cerebrospinal fluid as shown in Fig.1. Visual inspection of the extracted images shows that for the automatic brain extraction has succeeded quite well.

Image registration is often an essential step in the process from data acquisition to image analysis. After extracting the brains from the images, next phase is to register the AD patient and Control images to a common reference. During the registration process MNI152 template is used as a

target image. Advantages of using an MNI152 template for registration that it provides a reference that captures general variation of a population. First, source and target images are affinely registered with 12 degrees of freedom. The purpose of doing affine registration is to correct for global differences between the images. Then non-rigid image registration based on free-form deformation using B-spline approximation is performed. Image Registration Toolkit (ITK) was used in our work to perform the registrations[16, 27, 28]. During non-rigid registration process, choice of the spacing of the control points regulates the level at which the deformation takes place. In our approach, we have chosen a starting grid spacing of 20 mm, 10 mm and 5 mm respectively at three levels to find the non linear transformations.

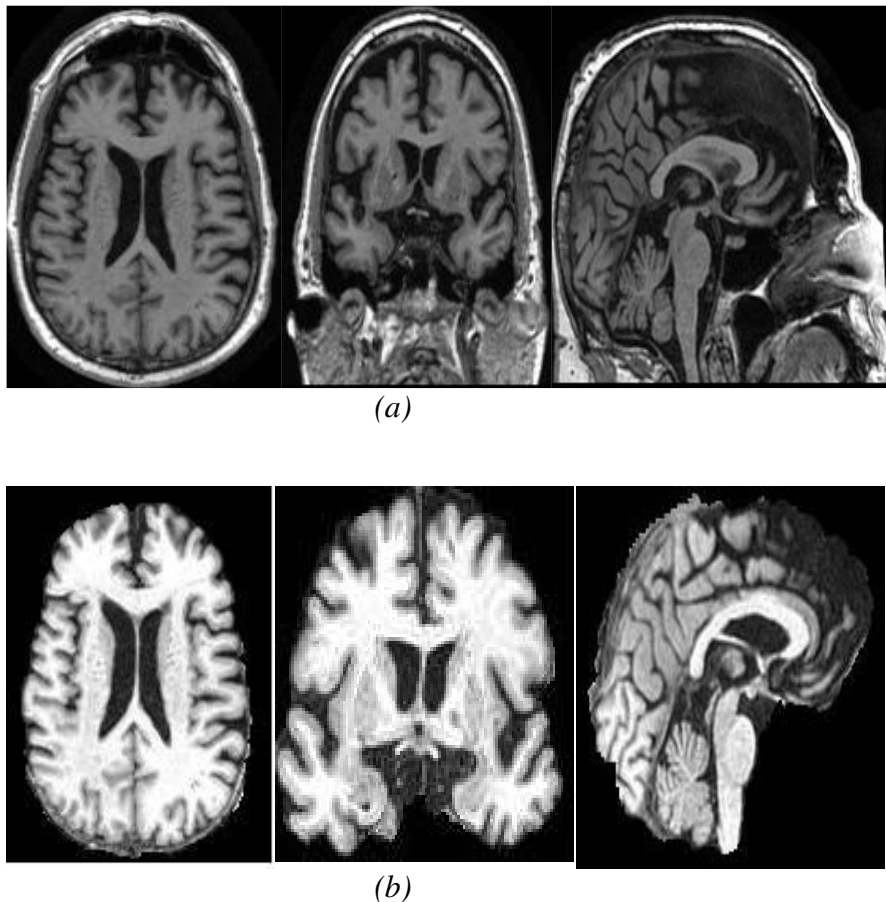


Fig.1. (a) Slices from a single MR image before brain extraction (b) After brain extraction

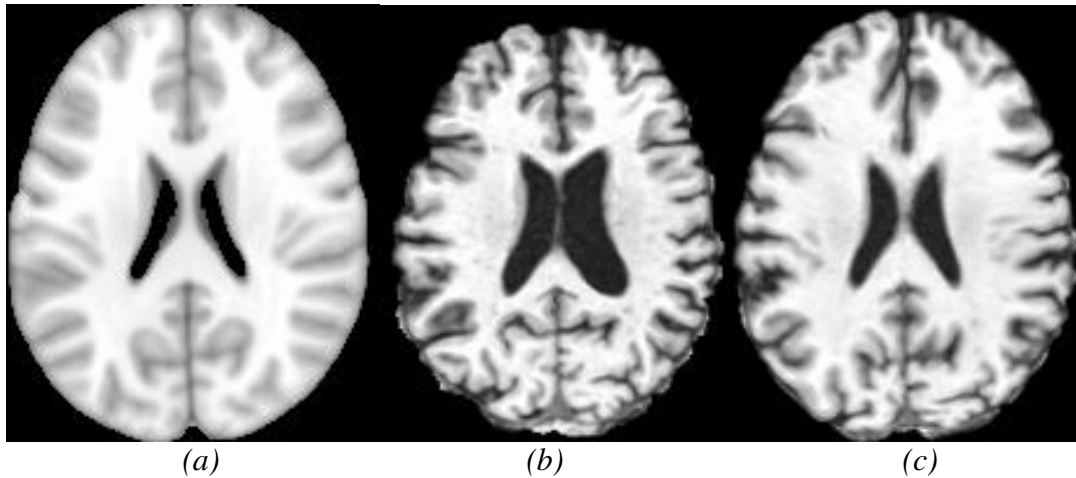


Fig.2. Subject 9 in (b) is registered to the target in (a). The result is shown in (c)

As shown in the Fig.2, the result of the affine registration and non-rigid registrations are visually inspected to ensure that the registration has succeeded. Inspection of the images shows that all the registrations are satisfactory.

The non-rigid registration produces the displacement values for each voxel in the image. The Jacobian operator is applied on the displacement field to visualize the relative volume change throughout the brain. Bright represents areas which are larger in the source than in the target, and vice versa for dark areas. A medium value (similar to background) represents no volume change. The slices from volumes of relative volumes obtained after Jacobian operator is shown in the Fig.3.

Voxelwise statistical analysis is performed to find statistically significant localized difference between two groups of subjects. Student t - test method with an alpha criterion of 0.05 is used for analysis of results. The resulting t values and p values from the t -test are further analyzed to identify the tissue volume change throughout the brain. The initial results indicate that the tissue volume change in the brain occurs predominantly in the hippocampus both in screening and 6 month time interval groups. The statistically significant differences found between AD and control group are shown in Fig.4 and Fig.5. Statistical maps with p values of screening data of the AD patients and controls is shown in Fig.6 and Fig.7.

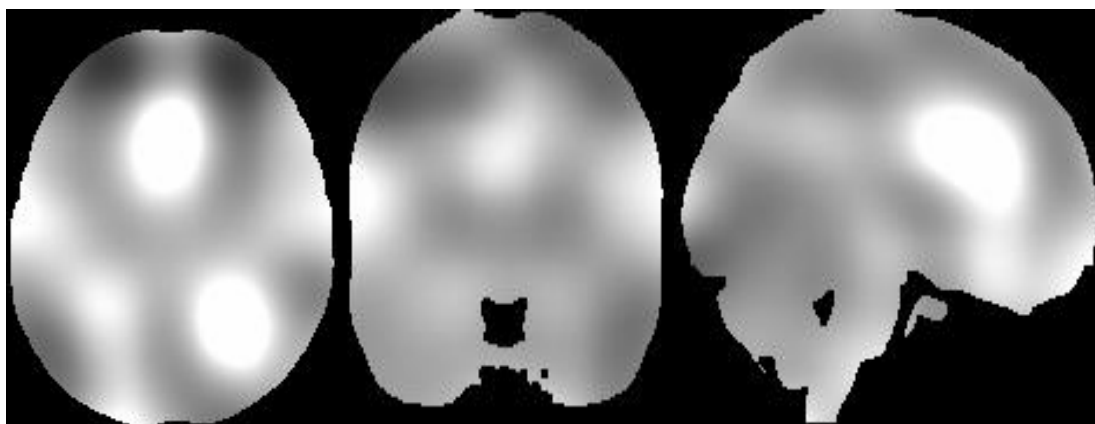


Fig.3. Slices of volume change per voxel subject 9.

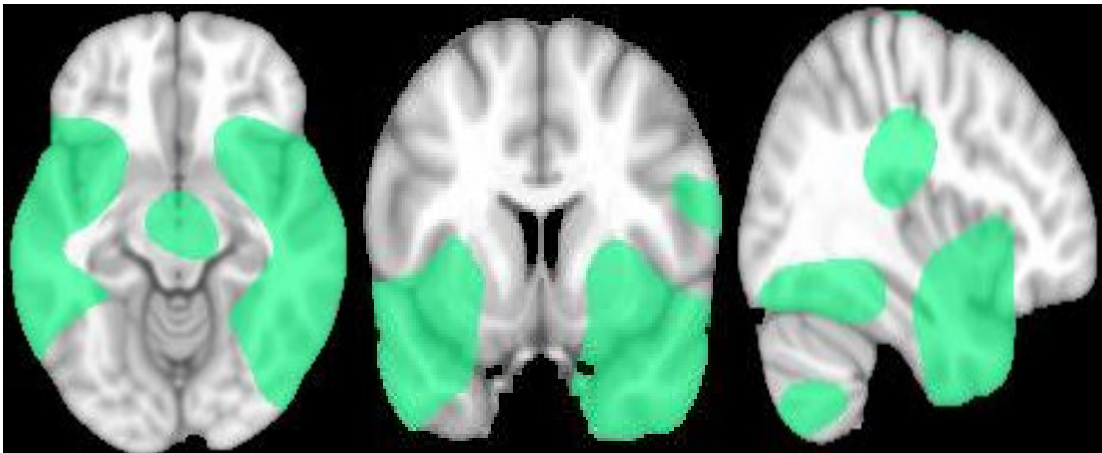


Fig.4. Statistically significant differences between screening data of AD patients and control group overlaid with anatomical data.

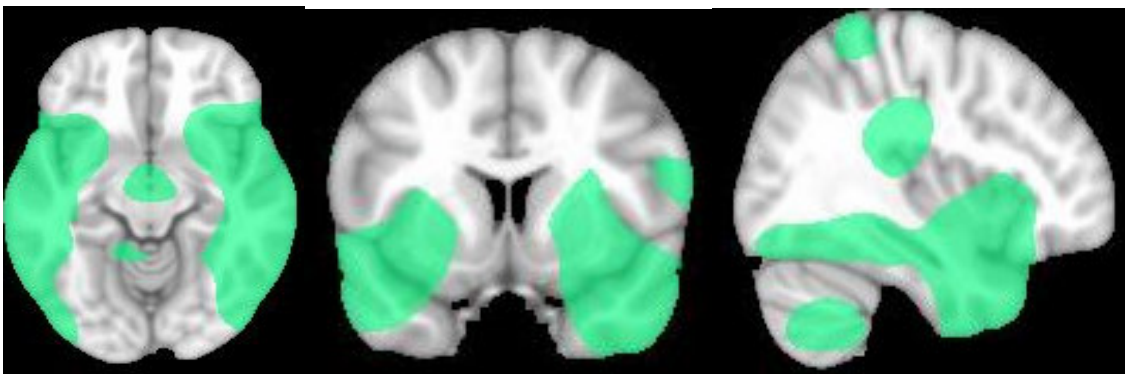


Fig.5. Statistically significant differences between 6 month time interval AD patients and control group overlaid with anatomical data

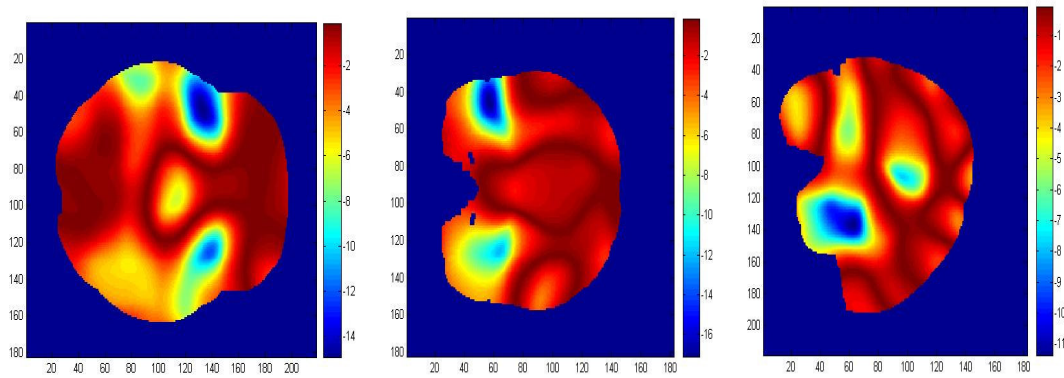


Fig.6. Statistical maps with p values ($p < 0.05$) of screening data of the AD patients and controls.

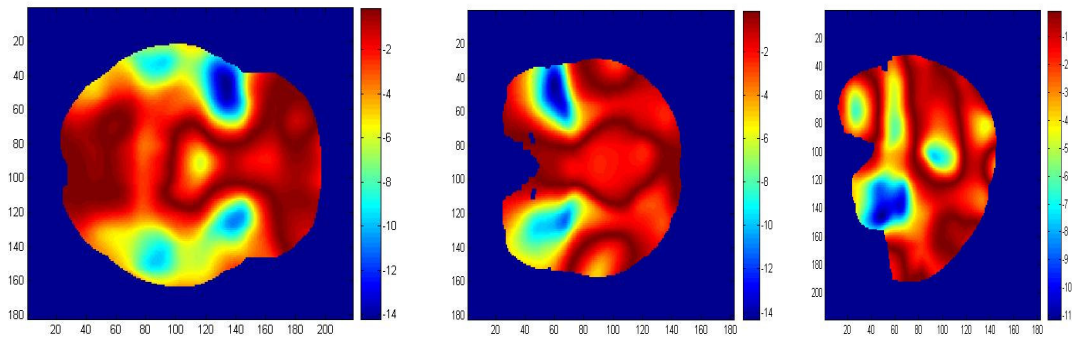


Fig.7. Statistical maps with p values ($p < 0.05$) of 6 month time interval AD patients and control

6 Conclusion

The main aim of the work is to analyze the deformation fields in Alzheimer's disease patients. The proposed work uses the techniques of image registration and Jacobian operator to analyze the brain tissue changes in Alzheimer's disease. For image registration, we have used affine registration to correct for global differences and non-rigid image registration based on free-form deformation using B-spline approximation. Further, 3D deformation fields are analyzed using student t-test. From our initial investigations, it has been found that a considerable amount of deformation in the brain occurs predominantly in the hippocampus both in screening and 6 month time interval groups. These differences between groups of subjects may be relevant to diagnosis, tracking of disease progression, and monitoring of potential disease-modifying treatments. In addition, brain tissue change may yield a more sensitive endpoint for diagnosing Alzheimer disease tracking its chronological progress in treatment trials and possibly for other neurodegenerative diseases. In future, along with structural magnetic resonance imaging, diffusion tensor imaging and other powerful analysis methods may be investigated to find clinically more useful information in mild cognitive impairment and Alzheimer's diseases.

Acknowledgments: The authors wish to thank Laboratory of Nuero Imaging, UCLA, for providing the ADNI dataset. We are indebted to Professor Risto Ilmoniemi and Mika Pollari, Laboratory of Biomedical Engineering, Helsinki University of Technology, Finland, for their valuable input, support and contribution to this work. The authors are grateful to the All India Council for Technical Education (AICTE), New Delhi, for the research grant # 8023/BOR/RPS-94/2006-07 under Research Promotion Scheme.

References:

- [1] Betke M, Hong H, and Ko J. P. Automatic 3D registration of lung surfaces in computed tomography scans, *Fourth International Conference on Medical Image Computing and Computer-Assisted Intervention*, Utrecht, Netherlands, 2001, pp.725–733.
- [2] Ghaffary B.K, Sawchuk A.A. A survey of new techniques for image registration and mapping, *Proceedings of the SPIE: Applications of Digital Image Processing*, 1983, pp.222–239.
- [3] Brown L.G. A survey of image registration techniques, *ACM Computing Surveys*, Vol. 24, 1992, pp. 326–376.
- [4] Maintz J.B.A, Viergever M.A. A survey of medical image registration, *Medical Image Analysis*, Vol. 2, 1998, pp. 1–36.

- [5] Torre-Ferrero C, Robla S, Sarabia E.G, Llata J.R. A Coarse-to-Fine Algorithm for 3D Registration based on Wavelet Decomposition, *WSEAS Transactions On Systems*, Vol. 7, 2008, pp. 655-664.
- [6] Emma Munoz-Moreno, Ruben Cardenes, Rodrigo De Luis-Garcia, Miguel Angel Martin-Fernandez, Carlos Alberola-Lopez, Image Registration Based on Automatic Detection of Anatomical Landmarks for Bone Age Assessment, *WSEAS Transactions On Computers*, Vol. 4, 2005, pp. 1596.
- [7] Ashburner J, Hutton C, Frackowiak R, Johnsrude I, Price C, Friston K. Identifying global anatomical differences: deformation-based morphometry, *Neuroimage*, Vol.6, 1998, pp.348-357.
- [8] Gaser C, Voltz H, Kiebel S, Riehemann S, Sauer H. Detecting structural changes in whole brain based on nonlinear deformations application to schizophrenia research, *Neuroimage*, Vol.10, 1999, pp.107-113.
- [9] Thompson P, Woods R, Mega M, Toga A. Mathematical/computational challenges in creating deformable and probabilistic atlases of the human brain. *Human Brain Mapping*, Vol.9, 2000, pp.81-92.
- [10] Pettey D, Gee J. Using a linear diagnostic function and non-rigid registration to search for morphological differences between populations: an example involving the male and female corpus callosum, *Proc SPIE Med Imaging*, Vol. 4322, 2001, pp.1636-1644.
- [11] Antoine Abche, Georges Tzanakos and E. Micheli-Tzanakou, Study of the Precision of a 3-D Image Registration Technique Using 3-D PET Brain Simulated Images, *WSEAS Transactions On Computers*, Vol. 4, 2, 2005, pp. 240.
- [12] Jack CR Jr, Slomkowski M, Gracon S, Hoover TM, Felmler JP, Stewart K, Xu Y, Shiung M, O'Brien PC, Cha R, Knopman D, Petersen RC. MRI as a biomarker of disease progression in a therapeutic trial of milameline for AD. *Neurolog*, Vol.60, 2003, pp.253-260.
- [13] Fox NC, Black RS, Gilman S, Rossor MN, Griffith SG, Jenkins L, Koller M. Effects of Abeta immunization on MRI measures of cerebral volume in Alzheimer disease, *Neurology*, Vol. 64, 2005, pp.1563-1572.
- [14] Zitova B, Flusser J. Image Registration Methods: A Survey, *Image and Vision Computing*, Vol.21, 2003, pp. 977-1000.
- [15] Sederberg T. W and Parry S. R. Free-form deformation of solid geometric models. In *Proceedings of SIGGRAPH '86, Computer Graphics*, 1992, pp.151-160.
- [16] Rueckert D, Sonoda L I, Hayes C, Hill D. L. G, Leach M O and Hawkes D. J. Non-rigid registration using free-form deformations: Application to breast MR images. *IEEE Transactions on Medical Imaging*, Vol.18, 1999, pp.712-721.
- [17] Feldmar J, Declerck J, Malandain G, and Ayache N. Extension of the ICP algorithm to non-rigid intensity-based registration of 3D volumes. *Computer Vision and Image Understanding*, Vol.66, 1997, pp.193-206.
- [18] Declerck J, Feldmar J, Goris M. L, and Betting F. Automatic registration and alignment on a template of cardiac stress and rest reoriented SPECT images. *IEEE Transactions on Medical Imaging*; Vol.6, 1997, pp. 727-737.
- [19] Denton E R E, Sonoda L I, Rueckert D, Rankin S C, Hayes C, Leach M, Hill D L G and Hawkes D J. Comparison and evaluation of rigid and nonrigid registration of breast mr images. *JCAT*, Vol.23, 1999, pp.800-805.
- [20] Foley J, van Dam A, Feiner S and Hughes J. *Computer Graphics*. Addison Wesley, 2nd edition, 1990.
- [21] Bookstein F. L., Principal warps: Thin-plate splines and the decomposition of deformations, *IEEE Trans. Pattern Anal. Machine Intell*, Vol.11, 1989, pp.567-585.

- [22] Davis M. H, Khotanzad A, Flamig D P and Harms S. E. A physics based coordinate transformation for 3-D image matching, *IEEE Transactions on Medical Imaging*, Vol.16, 1997, pp.317–328.
- [23] Davatzikos C. Spatial normalization of three-dimensional brain images using deformable models. *Journal of Computer Assisted Tomography*; Vol.20, 1996, pp.656– 665.
- [24] George W S and William G C. *Statistical Methods*. Iowa State University Press, 8th edition, 1989.
- [25] The Alzheimers disease Neuroimaging Initiative data set from Laboratory of Neuro Imaging, UCLA. Available: <http://www.loni.ucla.edu/ADNI>.
- [26] Smith S.M. Fast robust automated brain extraction. *Human Brain Mapping*; Vol.17, 2002, pp.143-155
- [27] Schnabel J. A, Rueckert D, Quist M, J. M. Blackall, A. D. Castellano Smith, T. Hartkens, G. P. Penney, W. A. Hall, H. Liu, C. L. Truwit, F. A. Gerritsen, D. L. G. Hill, and Hawkes D. J.. A generic framework for non-rigid registration based on non-uniform multi-level free-form deformations. *Fourth International Conference on Medical Image Computing and Computer-Assisted Intervention*, Utrecht, Netherlands, 2001, pp. 573-581
- [28] Studholme C, D.L.G.Hill, D.J. Hawkes, An Overlap Invariant Entropy Measure of 3D Medical Image Alignment, *Pattern Recognition*, Vol. 32, 1999, pp. 71-86.